JOURNAL OF MAGNETIC RESONANCE 68, 515–525 (1986)

Simulation of Two-Dimensional Cross-Relaxation Spectra in Strongly Coupled Spin Systems

LEWIS E. KAY,* J. N. SCARSDALE,† D. R. HARE, AND J. H. PRESTEGARD†

*Department of Molecular Biophysics and Biochemistry and †Department of Chemistry, Yale University, New Haven, Connecticut 06511

Received December 31, 1985; revised March 3, 1986

A two-dimensional NMR simulation program has been constructed which is capable of analyzing the effects of an arbitrarily complex sequence of hard pulses on a set of homonuclear spin-$\frac{1}{2}$ nuclei. The program is capable of simulating spin systems with strong J coupling and includes T_1 relaxation due to pair-wise dipolar interactions. In this capacity the program provides insight into the effects that strong coupling and dipolar spin–lattice relaxation can introduce in common 2D NMR experiments. As an illustration of the program, experimental and simulated NOESY data sets on 2,6-dicarboxynaphthalene are presented. Good agreement is found between the experimental and simulated spectra. Simulation of data sets with different mixing times, and different J couplings contributes to an understanding of the origin of deviations from first-order behavior.

INTRODUCTION

Two-dimensional NMR has become a valuable tool for providing structural and dynamic information on a wide range of molecules (*1–3*). Early applications, however, assumed spectra to be first order to achieve a simple interpretation of the position and magnitude of cross peaks in terms of molecular structure. As applications to more and more complex molecules have been pursued an understanding of deviations from simple first-order behavior and an understanding of new and more versatile 2D experiments have become increasingly important. This understanding often requires knowledge of phase properties of cross peaks (*4*) and second-order effects either from strong coupling (*5*) or complex relaxation pathways (*6*). In many cases, this knowledge cannot be obtained from the simple vector diagrams used to rationalize early pulse NMR experiments or the more recent spin operator formalism (*7, 8*). Often a more detailed solution in terms of density matrix methods is required. Density matrix manipulations are easily programmed on digital computers and the resulting programs can offer both insight into the effects of various components of a pulse sequence and simulation of expected results. Some versions of such programs have begun to appear (*9–11*).

We present here a program developed in our laboratory capable of simulating the effects of complex 2D pulse sequences on a homonuclear spin-$\frac{1}{2}$ system. The novel aspects of the program include its ability to simulate strongly coupled spin systems and the inclusion of T_1 relaxation due to spin-pair dipolar interactions. It is well

0022-2364/86 $3.00

known that strong coupling can give rise to intensity anomalies and additional resonances in 2D NMR spectra, and a computer program of this sort can provide insight into how significant these types of effects might be.

In this manuscript we will briefly review the requisite density matrix equations and give a short description of how the simulation program was constructed. In addition, we will present experimental and simulated 2D NOE spectra on 2,6-dicarboxynaphthalene, a small molecule which can be approximated as containing a pair of noninteracting, equivalent ABX spin systems.

THEORY

The density matrix equations necessary to describe the effects of arbitrarily complex pulse sequences on a weakly coupled, nonrelaxing spin system have been described by McClung *et al.* (*9*). We present here a similar approach which has been extended to include the effects of strong J coupling and T_1 relaxation.

The rotating-frame equation of motion of the density matrix, $\boldsymbol{\rho}(t)$, is given by

$$\frac{d}{dt}\boldsymbol{\rho} = \frac{i}{\hbar}[\boldsymbol{\rho}, \mathbf{H}]. \qquad [1]$$

In Eq. [1] we will initially treat only the effects of scalar coupling, chemical shift, and rf pulses so that

$$\mathbf{H} = \mathbf{H}_0 + \mathbf{H}_1 \qquad [2]$$

where $\mathbf{H}_0$ describes the interactions of the spins with the magnetic field in the rotating frame as well as J-coupling effects and $\mathbf{H}_1$ represents the contributions to $\mathbf{H}$ due to the application of an rf field.

The application of a strong pulse along axis $q(H_1 \gg H_0)$ allows straightforward integration of Eq. [1]. Representation of ρ at the end of the pulse is given by

$$\boldsymbol{\rho}(t^+) = \mathbf{R}_q(\theta)\boldsymbol{\rho}(t^-)\mathbf{R}_q^+(\theta) \qquad [3]$$

where

$$\mathbf{R}_q(\theta) = \exp(i\theta \sum_j \mathbf{I}_{qj}) \qquad [4]$$

is the pulse rotation operator in a basis set representation in which $\mathbf{H}_0$ is diagonal, $\mathbf{R}_q^+(\theta)$ is the matrix adjoint of $\mathbf{R}_q(\theta)$, and t^- and t^+ denote times immediately before and after application of the rf pulse, respectively.

Evolution of $\rho_{\alpha\beta}$ $(\alpha \neq \beta)$ during times when $\mathbf{H}_1 = 0$ can also be described in terms of a simple integrated form of Eq. [1]:

$$\rho_{\alpha\beta}(t) = \exp(i(\omega_\alpha - \omega_\beta)t)\rho_{\alpha\beta}(0)\exp(-t/T_2^*) \qquad [5]$$

where ω_α and ω_β are the appropriate eigenvalues of $\mathbf{H}_0$ containing chemical-shift and J-coupling information and $\rho_{\alpha\beta}(0)$ is the $\alpha\beta$ element of the density matrix after a pulse. Transverse relaxation is included as a single constant T_2^* for convenience in calculation. In general T_2^* will differ for different elements of the density matrix.

Pulse sequences are usually followed by observation of transverse magnetization. Once the time dependence of $\boldsymbol{\rho}$ is known, evaluation of transverse magnetization, $M_x + iM_y$, can proceed according to

$$M_x + iM_y = \gamma\hbar Tr\{\boldsymbol{\rho}(\mathbf{I}_x + i\mathbf{I}_y)\} \quad [6]$$

where $\mathbf{I}_q$ is the projection of spin angular momentum I along axis q in a basis set representation which diagonalizes $\mathbf{H}_0$.

The spin angular momentum matrices, $\mathbf{I}_x$ and $\mathbf{I}_y$, and the pulse rotation matrices, $\mathbf{R}_q(\theta)$, discussed above are generated for an N-spin case by a direct product recursive procedure similar to that used by McClung *et al.* in their simulation program (*9*). Transformation to a basis set representation which diagonalizes $\mathbf{H}_0$ is then accomplished according to

$$\mathbf{T}^{-1}\mathbf{O}\mathbf{T} \quad [7]$$

where $\mathbf{T}$ is a matrix of eigenvectors of $\mathbf{H}_0$ generated by standard matrix diagonalization subroutines and $\mathbf{O}$ is the matrix which is to be transformed from the direct product basis set to the basis set where $\mathbf{H}_0$ is diagonal. Calculation of magnetization at successive time points generates an FID which can be Fourier transformed to yield a frequency spectrum.

Introduction of spin relaxation into Eq. [1] is straightforward under certain limiting cases: namely, that we consider only spin–lattice relaxation, that we assume that all off-diagonal elements in $\boldsymbol{\rho}$ decay rapidly compared to T_1 ($T_2^* \ll T_1$) and that we work in a basis set that diagonalizes $\mathbf{H}_0$. Under these assumptions relaxation can be included by adding a single term to the diagonal elements of Eq. [1] so that they evolve according to (*12*)

$$\frac{d}{dt}\rho_{\alpha\alpha} = \sum_{\beta}{}' R_{\alpha\alpha\beta\beta}(\rho_{\beta\beta} - \rho^T_{\beta\beta}) \quad [8]$$

where $[\boldsymbol{\rho}, \mathbf{H}]_{\alpha\alpha} = 0$ since $\mathbf{H}_0$ is diagonal. In Eq. [8] $\rho^T_{\beta\beta}$ is the thermal equilibrium element of the density matrix corresponding to eigenvector $|\beta\rangle$. For a collection of n spins with $I = \frac{1}{2}$, $R_{\alpha\alpha\beta\beta}$ is an element of the $2^n \times 2^n$ Redfield T_1 relaxation matrix and is given by (*13*)

$$R_{\alpha\alpha\beta\beta} = \frac{1}{2\hbar^2}[2J_{\alpha\beta\alpha\beta}(\omega_\alpha - \omega_\beta) - \delta_{\alpha\beta}\sum_{\gamma} J_{\gamma\beta\gamma\alpha}(\omega_\gamma - \omega_\beta) - \delta_{\alpha\beta}\sum_{\gamma} J_{\gamma\alpha\gamma\beta}(\omega_\gamma - \omega_\beta)]. \quad [9]$$

In Eq. [9]

$$J_{\alpha\beta\gamma\delta}(\omega) = \int_{-\infty}^{\infty} \overline{\langle\alpha|H_d(t)|\beta\rangle\langle\delta|H_d(t+\tau)|\gamma\rangle}\exp(-i\omega\tau)d\tau \quad [10]$$

where $H_d(t)$ is the dipolar Hamiltonian at time t, $\{|\alpha\rangle\}$ is the set of eigenvectors of $\mathbf{H}_0$, $\delta_{\alpha\beta}$ is the Kroenecker delta function, and the bar denotes an ensemble average.

In our simulation we will zero the off-diagonal elements of $\boldsymbol{\rho}$ at the onset of specified relaxation periods. This eliminates cross-peaks which arise due to the excitation of all orders of coherence by the 90°–t_1–90° portion of the NOESY sequence. Experimentally this is achieved by a stochastic variation of the mixing time or by application of a gradient pulse at the start of the mixing period (*14*). The assumptions used in modifying Eq. [1] are in keeping with our primary objective of providing an assessment of the contributions of strong J coupling to NOE spectra. These contributions are distinct from the effects that give rise to the zero and high-order quantum J peaks discussed by Ernst *et al.* (*14*) and will be elaborated on in the discussion.

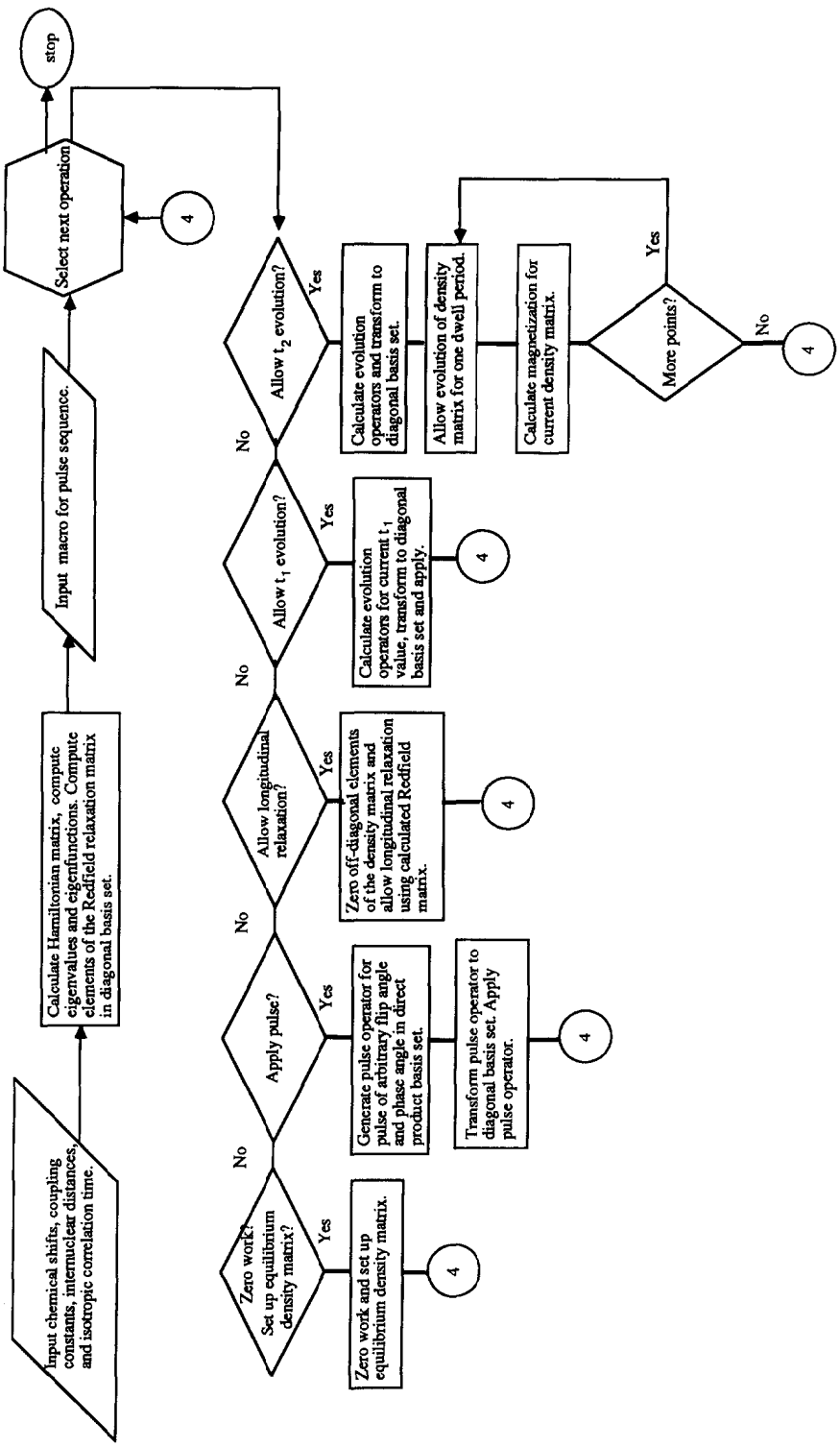

FIG. 1. Flow chart showing the construction of the spectral simulation program.

Evolution during a mixing or relaxation period can now be treated using Eq. [8] which can be integrated to give

$$\rho(t) = \rho^T + \mathbf{Q}[\exp(\mathbf{Q}^{-1}\mathbf{R}\mathbf{Q})t]\mathbf{Q}^{-1}(\rho(0)-\rho^T) \quad [11]$$

where $\rho(t)$ and ρ^T are column vectors containing the on-diagonal elements of the density matrix at time t after the start of the relaxation period and at equilibrium, respectively, **R** is the Redfield T_1 relaxation matrix, and **Q** is a matrix containing the eigenvectors of **R**.

Elements of the Redfield T_1 relaxation matrix describing relaxation due to pairwise dipolar interactions between spins were obtained by expressing the wavefunctions of the spin system as linear combinations of the simple product wavefunctions using coefficients determined by the eigenvectors of the Hamiltonian. $R_{\alpha\alpha\beta\beta}$ was then calculated using Eqs. [9] and [10] and assuming isotropic motion.

Figure 1 shows a flow chart illustrating the implementation of the simulation scheme described above. The program was written in Fortran and was run on a Vax 11/750 computer making use of a CSPI Minimap array processor for most matrix manipulations. Because the program has the capability of phase cycling both receiver and pulse phases independently it is possible to carry out 2D simulations in quadrature in both dimensions or to phase cycle to remove artifacts such as strong axial peaks generated in 2D NOE experiments.

RESULTS

To test the program we have chosen to simulate a NOESY experiment on a molecule of 2,6-dicarboxynaphthalene. The pulse sequence simulated in this study is $(90°)\phi_1$–t_1–$(90°)\phi_2$–τ–$(90°)\phi_3$–t_2 in which $(90°)\phi_i$ is a hard rf pulse of phase ϕ_i, t_1 is the evolution time, τ is the mixing period, and t_2 is the acquisition period. The spin system simulated was represented as a three-spin ABX case. A 1D spectrum of the molecule shows strong scalar coupling between protons 3 and 4. Strong dipolar interactions exist between ^{1}H(3) and ^{1}H(4) and between ^{1}H(4) and ^{1}H(5) with a weaker interaction existing between ^{1}H(3) and ^{1}H(5). In Fig. 2 the A spin is assigned to ^{1}H(3) while the B and X spins are assigned to protons 4 and 5, respectively. Shifts and coupling constants are summarized in Table 1. Internuclear distances were obtained from a crystal structure of napthalene (*15*). The correlation time used in the simulation experiments was calculated using the T_1 value of proton 5 and assuming that its only source of relaxation is due to strong dipolar coupling with proton 4.

Figure 3a shows a simulated NOE experiment of protons 3, 4, 5 of the molecule

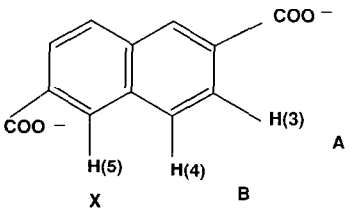

FIG. 2. Molecular structure of 2,6-dicarboxynaphthalene.

TABLE 1

Spectral Simulation Parameters

Chemical shift (ppm)	Internuclear distance (nm)	Coupling constants (Hz)
$\delta_3 = 7.91$	$r_{34} = 0.244$	$J_{34} = 8.53$
$\delta_4 = 7.99$	$r_{45} = 0.248$	$J_{45} < 0.7$
$\delta_5 = 8.36$	$r_{35} = 0.475$	$J_{35} < 0.7$

2,6-dicarboxynaphthalene with phase cycling to eliminate axial peaks. The carrier was placed at one end of the spectrum since the set was not simulated with quadrature in T_1. Two hundred fifty-six experiments each containing 256 points were generated.

Figure 3b shows the experimental 2D NOESY spectrum of 2,6-dicarboxynaphthalene at 298 K. 2,6-Dicarboxynaphthalene (dipotassium salt, Aldrich, Milwaukee, Wis.) was dissolved in D_2O to give a concentration of 0.05 *M* and the sample was purged with N_2 for 5 min before sealing. EDTA (5 m*M*) was added to scavenge any paramagnetic impurities in the sample. The data were acquired on a 250 MHz spectrometer operating in the pulse Fourier transform mode. A 16 scan pulse sequence which suppresses axial peaks as well as double quantum coherence and allows for quadrature in F_1 (*n* type) and F_2 was employed. A mixing delay of 3 s was chosen and was varied stochastically to eliminate *J* cross peaks. One hundred twenty-eight experiments with 128 complex points per experiment were acquired. A sweep width of 300 Hz was employed to give the same resolution as in the simulated spectra. Both data sets were symmetrized.

Figures 4 and 5 show column cross-sections through resonances centered at $\delta = 8.36$ ppm and $\delta = 7.89$ ppm, respectively, from both simulated (a) and experimental (b) data sets.

Both the experimental and the theoretical data sets were processed on a Vax 11/750 computer. In both cases the data were weighted by using the sine-bell weighting function on all points in both dimensions, magnitude corrected, and zero-filled to give a 1K by 1K matrix.

DISCUSSION

Figures 3, 4, and 5 show good qualitative agreement between the simulated and the theoretical NOESY spectra of 2,6-dicarboxynaphthalene. A good representation of the one-dimensional spectrum exists on the diagonal of Fig. 3 with A, B, and X peaks at 7.91, 7.99, and 8.36 ppm relative to HDO. Cross peaks between protons 3 and 4 and protons 4 and 5 expected based on first-order analysis and the spatial proximity of the spins (2.44 and 2.45 Å) are seen at (7.99 ppm, 7.91 ppm), (7.91 ppm, 7.99 ppm) and (8.36 ppm, 7.99 ppm), (7.99 ppm, 8.36 ppm), respectively. A comparison of cross-peak intensity ratios is presented in Table 2. We believe that there is good agreement between simulated and experimental data sets. The deviations observed very likely result from small errors in the internuclear distances input into the simulation program. These distances were obtained from a refined crystal structure of napthalene (*15*) in which proton positions were calculated based on idealized geometries. For distances on the order of 2.5 Å, an error of 5–10% can account for the

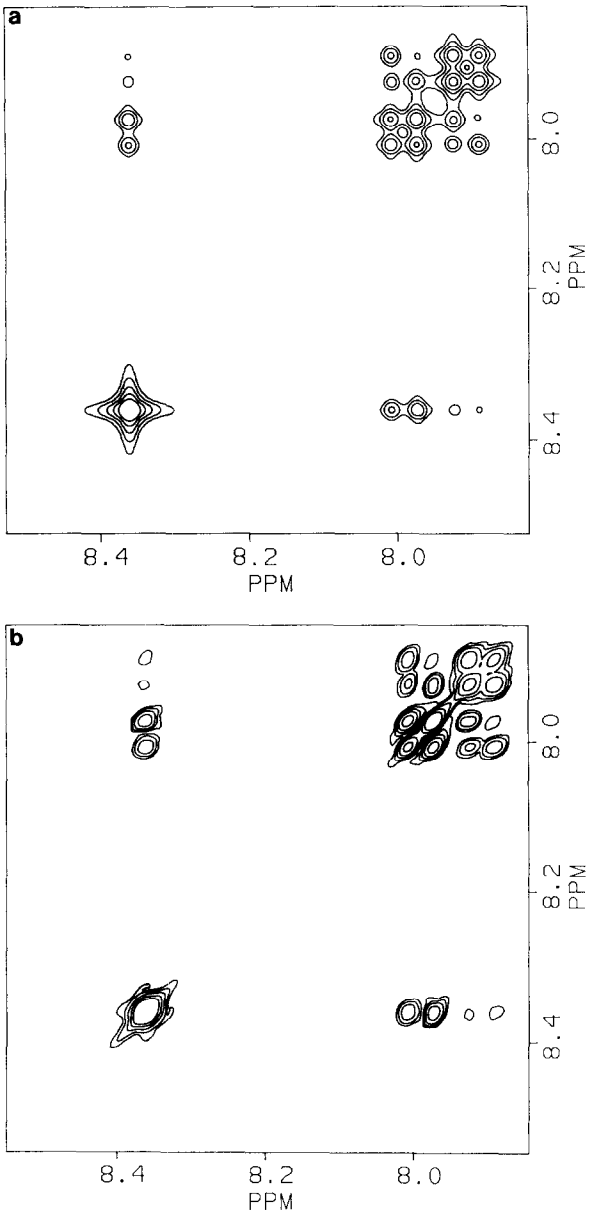

FIG. 3. (a) Contour plot of a simulated 2D NOE experiment on an ABX spin system using parameters summarized in Table 1. (b) Contour plot of an experimental 2D NOE experiment on 2,6-dicarboxynaphthalene using sweep widths and spectral parameters to correspond to those in a.

discrepancies between experiment and theory observed in this study. Other possible sources of discrepancy between experimental and simulated data sets come about due to the neglect of cross-correlation terms in expressions for the elements of the Redfield relaxation matrix and the assumption of isotropic motion.

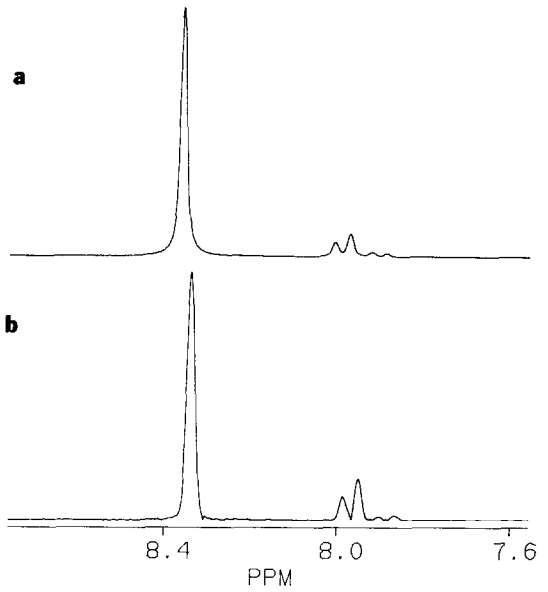

FIG. 4. Simulated (a) and experimental (b) column cross-section through resonance centered at $\delta = 8.36$ ppm.

One of the important features of the simulation program lies in its capacity to evaluate the relative importance of different pathways of magnetization transfer. For example, the transfer of magnetization from $^1H(3)$ to $^1H(4)$ can originate in one of two different processes. The first process, which is well understood, is an incoherent

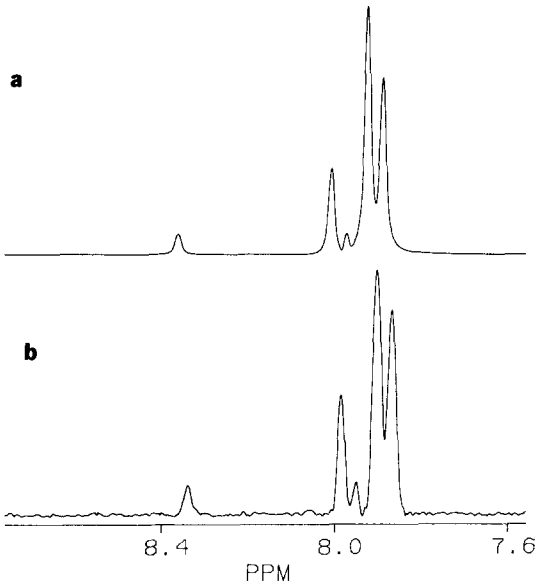

FIG. 5. Simulated (a) and experimental (b) column cross-section through resonance centered at $\delta = 7.89$ ppm.

TABLE 2

Intensities of Selected Column Cross-Sections

Column cross-section	δ Cross-section resonance	Observed intensity	Simulated intensity
$\delta = 8.36^b$	8.36	1	1
	7.99[a]	0.18	0.12
	7.90[a]	0.028	0.026
$\delta = 7.89^c$	8.36	0.060	0.044
	8.01	0.23	0.22
	7.97	0.060	0.044
	7.91[a]	1	1

[a] Integrated intensity of the doublet.
[b] Data normalized to singlet at $\delta = 8.36$ ppm.
[c] Data normalized to doubled centered at $\delta = 7.91$ ppm.

transfer due to cross-relaxation between the interacting spins. This transfer is distance dependent and is the one assumed to be operative in attempting a first-order analysis in terms of molecular structure. The second transfer process arises purely from scalar coupling and is distance independent. Its neglect can lead to errors in structure analysis. This latter effect is due to unequal mixing of elements of transverse magnetization into longitudinal magnetization by the $90°$–t_1–$90°$ excitation sequence. Ernst *et al.* have shown that for a weakly coupled two-spin-$\frac{1}{2}$ system on-diagonal elements of the density matrix differing in the spin state of the first nucleus (e.g., $\langle\alpha\alpha|\rho|\alpha\alpha\rangle$ and $\langle\beta\alpha|\rho|\beta\alpha\rangle$) at the beginning of the mixing period contain equal intensity contributions from magnetization evolving during t_1 at the characteristic frequency of the second nucleus (*14*). A third $90°$ pulse produces magnetization associated with the first spin, proportional to the difference of such on-diagonal elements. Because of the equality of these elements no modulation at frequencies corresponding to the transition of the second nucleus would occur. Strong coupling removes the equality between such elements so that in general some of the on-diagonal elements associated with the first spin in the weak coupling case now contain different mixtures of frequency labeled components of the second spin. Application of the third $90°$ pulse samples this inequality so that, for a two-spin system, an element of transverse magnetization in t_2 will be a function of all four frequency labeled components in t_1. The effects produced are somewhat analogous to the transfer of magnetization which occurs in spin systems containing resolvable J couplings which are excited with a pulse sequence of the form $(90°)\phi_1$–t_1–$(\beta)\phi_2$–τ–$(\beta)\phi_3$–t_2 with $\beta \neq \pi/2$ (*16*). In this case the first β pulse partly converts out-of-phase magnetization, $2I_{ky}I_{lz}$, into longitudinal two-spin order, $2I_{kz}I_{lz}$, which is subsequently converted into observable antiphase magnetization, $2I_{ky}I_{lz}$ and $2I_{ly}I_{kz}$, by the second β pulse (see Eq. [3] of (*16*)). In this way transverse magnetization associated with spin k can be transferred to spin l even in the limit where τ is small compared to the inverse of the cross-relaxation rate. The latter mechanism, however, is inoperative when β is set equal to $90°$.

Contributions from these different processes can be evaluated by simulating spectra

under certain limiting conditions. For example, by setting the mixing time to zero we eliminate the dipolar mechanism of magnetization transfer between spins 3 and 4. In this way, we have determined that 30% of the magnetization transferred between ^{1}H(4) and ^{1}H(3) occurs via cross-relaxation between these spins. The remaining 70% is therefore attributed to the scalar coupling mechanism. This is not surprising in lieu of the highly second-order nature of the ^{1}H 3–4 spin system ($J/\delta = 0.44$). In experimental situations departures from first-order behavior are easily recognized. For example, the multiplet components of the cross peaks centered at (7.91, 7.99) and (7.99, 7.91) are highly asymmetric. In first order all four components of the cross peaks should have equal intensity.

The appearance of cross peaks between protons 3 and 5 clearly cannot be interpreted on a first-order basis since protons 3 and 5 are 4.75 Å apart and first-order cross-relaxation mechanisms should account for less than 10% of the ^{1}H(5) to ^{1}H(3) cross-peak intensity. Understanding the origin of the additional intensity is important in avoiding misassignment and misinterpretation. ^{1}H(5) to ^{1}H(3) magnetization transfer originates in any one of several different second-order processes including the following: (1) Magnetization transferred from ^{1}H(5) to ^{1}H(4) by cross-relaxation can be transferred by a successive cross-relaxation step from ^{1}H(4) to ^{1}H(3). Successive through-space transfers are more important for large molecules where T_2 relaxation is more efficient than T_1 relaxation (spin diffusion limit) but they can produce finite effects here. (2) Magnetization transferred between protons 5 and 4 appears associated with proton 3 because of the strong J coupling between protons 4 and 3. This strong coupling effect mixes the zero-order wavefunctions of 4 and 3 so that the eigenstate of proton 3 is some linear combination of the zero-order eigenstates of protons 4 and 3. In this way a fraction of magnetization transferred between protons 5 and 4 contributes to the resonances associated with proton 3.

It is possible to evaluate the efficiency of the second-order transfer processes contributing to the cross peaks between ^{1}H(5) and ^{1}H(3) by setting various scalar couplings to zero. Setting $J_{34} = 0$ allows an assessment of the relative contribution of the second transfer process discussed above. When this is done, the cross peak at $F_1 = 8.36$ ppm, $F_2 = 7.91$ ppm, corresponding to magnetization originating on spin 5 and residing during t_2 on spin 3, decreases by 45%. Hence process (1) contributes 55% of the intensity of this second-order cross peak while the latter process contributes the remaining 45%.

Apportionment of magnetization to different mechanisms as discussed above can lead to a better understanding of second-order effects in NOESY-type spectra and proper utilization of cross-peak intensities in geometric analysis.

ACKNOWLEDGMENTS

This work was supported by Grant GM-33225 from the National Institutes of Health, by predoctoral fellowships to L.E.K. from the Natural Sciences and Engineering Research Council of Canada, and from the Heritage Trust Fund of Alberta, Canada, and by a predoctoral fellowship to J.N.S. from the National Science Foundation. The research benefited from instrumentation provided through shared instrumentation programs of the National Institute of General Medical Science, GM 3224351, and the Division of Research Resources of NIH, RR02379. We thank Maureen O'Brien for her assistance with some aspects of this work.

REFERENCES

1. A. BAX, *in* "Two Dimensional Nuclear Magnetic Resonance in Liquids," Delft Univ. Press, Dordrecht, Holland, 1982.
2. G. WIDER, S. MACURA, A. KUMAR, R. R. ERNST, AND K. WÜTHRICH, *J. Magn. Reson.* **56,** 207 (1984).
3. M. P. WILLIAMSON, T. F. HAVEL, AND K. WÜTHRICH, *J. Mol. Biol.* **182,** 295 (1985).
4. D. NEUHAUS, G. WAGNER, M. VASAK, J. H. R. KAGI, AND K. WÜTHRICH, *Eur. J. Biochem.* **151,** 257 (1985).
5. G. WIDER, R. BAUMANN, K. NAGAYAMA, R. R. ERNST, AND K. WÜTHRICH, *J. Magn. Reson.* **42,** 73 (1981).
6. A. A. BOTHNER-BY AND T. H. NOGGLE, *J. Am. Chem. Soc.* **101,** 5152 (1979).
7. O. W. SØRENSEN, G. W. EICH, M. H. LEVITT, G. BODENHAUSEN, AND R. R. ERNST, *Prog. NMR Spectrosc.* **16,** 163 (1983).
8. F. T. M. VAN DE VEN AND C. W. HILBERS, *J. Magn. Reson.* **54,** 512 (1983).
9. B. K. JOHN AND R. E. D. MCCLUNG, *J. Magn. Reson.* **58,** 47 (1984).
10. G. BODENHAUSEN, R. FREEMAN, G. A. MORRIS, AND D. L. TURNER, *J. Magn. Reson.* **31,** 75 (1978).
11. M. A. THOMAS AND A. KUMAR, *J. Magn. Reson.* **56,** 479 (1984).
12. H. SHIMIZU AND S. FUJIWARA, *J. Chem. Phys.* **34,** 1501 (1961).
13. A. G. REDFIELD, *IBM J.* **1,** 19 (1957).
14. S. MACURA, Y. HUANG, D. SUTER, AND R. R. ERNST, *J. Magn. Reson.* **43,** 259 (1981).
15. D. W. J. CRUICKSHANK, *Acta Cryst.* **10,** 504 (1957).
16. G. BODENHAUSEN, G. WAGNER, M. RANCE, O. W. SØRENSEN, K. WÜTHRICH, AND R. R. ERNST, *J. Magn. Reson.* **59,** 542 (1984).